

EXPLORING FUNCTIONAL BRAIN DYNAMICS VIA A BAYESIAN CONNECTIVITY CHANGE POINT MODEL

Zhichao Lian^{1*}, Xiang Li^{2*}, Jianchuan Xing^{4,1}, Jinglei Lv², Xi Jiang², Dajiang Zhu², Shu Zhang², Jiansong Xu³, Marc N. Potenza³, Tianming Liu^{2**}, Jing Zhang^{1**}

¹Department of Statistics, Yale University, New Haven, CT; ²Cortical Architecture Imaging and Discovery Lab, Department of Computer Science, University of Georgia, Athens, GA; ³Department of Psychiatry, Yale University, New Haven, CT; ⁴School of Computer Science and Engineering, University of Electronic Science and Technology of China, Chengdu, P.R. China.

*Joint first authors, **Joint corresponding authors.

ABSTRACT

Multiple recent neuroimaging studies have demonstrated that the human brain's function undergoes remarkable temporal dynamics. However, quantitative characterization and modeling of such functional dynamics have been rarely explored. To fill this gap, we presents a novel Bayesian connectivity change point model (BCCPM), to analyze the joint probabilities among the nodes of brain networks between different time periods and statistically determine the boundaries of temporal blocks to estimate the change points. Intuitively, the determined change points represent the transitions of functional interaction patterns within the brain networks and can be used to investigate temporal functional brain dynamics. The BCCPM has been evaluated and validated by synthesized data. Also, the BCCPM has been applied to a real block-design task-based fMRI dataset and interesting results were obtained.

Index Terms— fMRI, graph model, change point detection

1. INTRODUCTION

Recent neuroscience research indicates that dynamic interactions between connections from higher to lower-order cortical areas and intrinsic cortical circuits involve moment-by-moment functional switching in brain [1], and the brain may undergo a succession of states when performing a task, with each state serving as a source of top-down influences for subsequent states [1]. It has been reported that functional connectivities are under dynamic state changes at different time scales [2], and there have been accumulating studies analyzing brain functional dynamics, including statistical methods such as Hierarchical Exponentially Weighted Moving Average (HEWMA) method on fMRI signals to detect BOLD signal state change in response to stimulus [3], and sliding-time window based approaches to capture the dynamics of functional brain interactions [4].

Specifically, the estimation of functional brain state-related change points without a prior timing information has been an important consideration, as in many cases psychological processes could not be specified in advance

[3]. Also, as the onset time and the duration of the response may vary considerably across subjects [3], it would be reasonable and possibly advantageous to model the brain's functional dynamics by the intrinsic changes in their functional interaction patterns. Previous studies have suggested that multivariate graphical causal models based on Bayesian networks are more robust and reliable in estimating functional interactions and less sensitive to noise in the fMRI signals [5]. Thus in this work, we have developed a novel Bayesian connectivity change point model (BCCPM) to analyze the dynamics of multivariate functional interactions and infer the boundaries of temporal blocks via a unified Bayesian framework. We have applied the proposed model on a working memory task-based fMRI dataset defined on common structural connectomes that are constructed from DTI data via the publicly available DICCCOL (Dense Individualized and Common Connectivity-Based Cortical Landmarks) system [6]. Compared with existing fMRI time series changes [11], pair-wise functional connectivity changes [12] or sliding-window based framework [16], a key conceptual novelty in the BCCPM is that the change point in fMRI time series is defined as an abrupt change of multivariate functional interactions in brain networks. The major methodological novelty is that the proposed model is capable of capturing the changes of multivariate functional interactions via a Bayesian framework. Compared to the Dynamic Connectivity Regression (DCR) method in [14], our proposed model is able to handle a large number of variables efficiently. Therefore, quantitative investigation of multivariate functional interaction dynamics within whole brains will become possible and feasible, as shown in our later experiments results.

2. METHOD

2.1. Data acquisition

In this study, we applied the BCCPM to a working memory task-based fMRI dataset for validation and in order to test its practical applicability. FMRI datasets of 10 participants were acquired during a modified version of an operational span (OSPAN) task [7] on a 3T GE

Signa scanner. The total scan length was 540 seconds with TR of 2 seconds, resulting in a dataset consisting of 270 volumes (i.e., time points). Preprocessing steps were based on FSL, and additional details could be found in our previous work [7]. We used 358 DICCCOL ROIs (Regions of Interest) of each subject's brain via the publicly available open-source tools in [6] and extracted the fMRI signals. It should be noted that the DICCCOLs have intrinsic correspondences across individuals [6], thus enabling us to compare results across different subjects. For each subject, the fMRI dataset is a 270*358 time series matrix measuring the brain activity of 358 ROIs over the whole 270-volume time period.

2.2. Bayesian connectivity change point model

Given a set of vectors x_1, x_2, \dots, x_T i.i.d. (independent and identically distributed) from the m -dimensional multivariate normal distribution $x_t \sim N(\mu, \Sigma)$ $t=1, 2, \dots, T$, where T denotes the number of vectors, m denotes the dimension of vector x_t , μ denotes the m -dimensional mean vector, and Σ denotes the $m \times m$ covariance matrix. The conjugate prior distribution of (μ, Σ) is the $N-Inv-Wishart(\mu_0, \Lambda_0 / \kappa_0, \nu_0, \Lambda_0)$ [8] and the posterior distribution of (μ, Σ) based on the data x_1, x_2, \dots, x_T is $N-Inv-Wishart(\mu_T, \Lambda_T / \kappa_T, \nu_T, \Lambda_T)$. Thus, we calculate the probability of x_1, x_2, \dots, x_T as follows [8]:

$$P(x_1, \dots, x_T) = \frac{P(x_1, \dots, x_T | \mu, \Sigma)}{P(\mu, \Sigma | x_1, \dots, x_T)} = \left(\frac{1}{2\pi}\right)^{mT/2} \left(\frac{\kappa_0}{\kappa_T}\right)^{m/2} \frac{\Gamma_m\left(\frac{\nu_T}{2}\right) (\det(\Lambda_0))^{\nu_0/2}}{\Gamma_m\left(\frac{\nu_0}{2}\right) (\det(\Lambda_T))^{\nu_T/2}} 2^{mT/2} (1)$$

where Γ_m is the multivariate gamma function:

$$\Gamma_m(z) = \pi^{m(m-1)/4} \prod_{j=1}^m \Gamma(z + (1-j)/2). \quad (2)$$

Given an $m \times T$ ROI data matrix $\mathbf{X} = (x_1, x_2, \dots, x_T)$ (here T denotes the number of observations in the temporal order and m denotes the number of ROIs) as illustrated in the sample matrix (Fig. 1a), we are interested in the change points where there are underlying differences in the joint probabilities (defining functional interactions) among the m ROIs between different time periods. Fig. 1b illustrates the basic ideas of the proposed BCCPM, where one change point located at time point 101 partitioned three fMRI time series into two different functional interaction patterns.

We define a block indicator vector $\vec{I} = (I_1, \dots, I_T)$, where $I_t=1$ if the t -th observation x_t is a change point (defined as the starting point of a temporal block), $I_t=0$ otherwise. Then the T temporal observations would be segmented into totally $\sum_{t=1}^T I_t$ blocks, as the starting time

point I_t is always considered as a change point. The likelihood of the data matrix $\mathbf{X} = (x_1, x_2, \dots, x_T)$ is:

$$p(\mathbf{X} | \vec{I}) = \prod_{b=1}^{\sum I_t} p(\mathbf{X}_b) \quad (3)$$

\mathbf{X}_b is the temporal observations belonging to b -th block and $p(\mathbf{X}_b)$ could be calculated according to Eq. 1. The temporal blocks are independent from each other, therefore the posterior distribution of the configuration is:

$$p(\vec{I} | \mathbf{X}) \propto p(\vec{I}) \cdot p(\mathbf{X} | \vec{I}) \quad (4)$$

where $p(\vec{I}) = \prod_{t=1}^T p(I_t)$ and $p(I_t) \sim \text{Bern}(0.5)$.

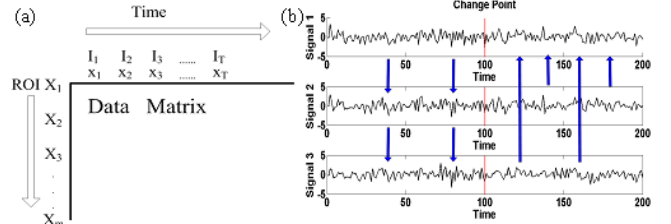


Fig. 1 (a) Illustration of data matrix of \mathbf{X} and block indicator vector \vec{I} , where x_t are the values of all ROIs at time t (the t -th column in the matrix), X_j are the values of the j -th ROI at all times (the j -th row in the matrix) and I_t is the block indicator (defining the change points) for time t ; (b) Signals of three ROIs with one temporal change point at 101. The functional interaction pattern among 3 fMRI signals changes from signal1 \rightarrow signal2 \rightarrow signal3 to signal2 \rightarrow signal1 \leftarrow signal3.

We use the Metropolis-Hastings scheme [9] to sample the posterior distribution $p(\vec{I} | \mathbf{X})$ with a random initial block indicator vector i^0 . For the n -th ($n > 0$) iteration:

1. Propose a new block indicator vector \vec{I}^* by randomly choosing an indicator in \vec{I}^{n-1} and changing its value from 0 to 1 or from 1 to 0.
2. Evaluate $p(\vec{I}^* | \mathbf{X})$ according to Eq. 4.
3. Generate a uniformly distributed random number u from range (0, 1) and set:

$$\vec{I}^n = \begin{cases} \vec{I}^* & \text{if } u \leq \min \left[1, \frac{p(\vec{I}^* | \mathbf{X})}{p(\vec{I}^{n-1} | \mathbf{X})} \right] \\ \vec{I}^{n-1} & \text{otherwise} \end{cases} \quad (5)$$

4. Iterate until n reaches a given number N (in our simulation, N is set as 2000 to make sure that $p(\vec{I}^n | \mathbf{X})$ converges).
5. Finally, the burn-in is excluded from the actual MCMC sample of the posterior distribution and then the posterior probability for each time point to be a change point is calculated from MCMC samples.

3. RESULTS

3.1. Simulation results

In this section, simulation data were generated by two different models to evaluate and validate the proposed BCCPM. In the first model, six different networks with dynamic structures were generated, which are illustrated in the top panels in Fig. 2 and the posterior probabilities for each time point as the change point are illustrated in the bottom panels.

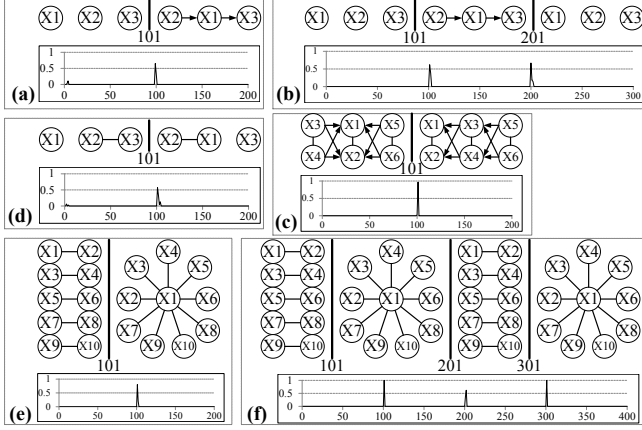


Fig. 2 Change point detection results of six dynamic networks.

Taking the 5th network as an example (shown in Fig. 2e), we generated 10 ROIs (X1 to X10) and 200 time points comprising of two 100-volume blocks, where in the first block from time point 1 to 100, all 5 pairs of 10 ROIs are independent of each other. Within each pair, two ROIs are $\sim N(0, \Sigma)$, $\Sigma = \begin{pmatrix} 1 & 0.8 \\ 0.8 & 1 \end{pmatrix}$.

In the second block from time point 101 to 200, the network is a star-like structure, with X1 being the center and other ROIs (X2 to X10) dependent on it with correlation coefficient $\rho=0.8$. This star-like structure means given X1, all other ROIs (X2 to X10) are conditionally independent of each other. From the bottom panels in Figs. 2a-2f, it can be seen that the proposed BCCPM accurately detected all of the changes points from all of the models. In addition, we repeated the simulations 100 times and obtained very low average type I error rate (1.67%) and type II error rate (0.83%).

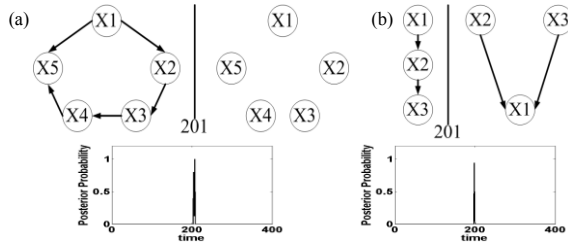


Fig. 3 Change point detection results of two dynamic networks.

In the second simulation, two sets of time series on different nodes were generated based on a well-accepted network modeling method proposed by Smith et al. [10]. Fig. 3 visualizes the dynamic interaction patterns of

these two time series, and the proposed BCCPM detected change points in both models accurately. Further, we repeated the simulation 50 times and the results further validated the good performance of BCCPM (the average Type I error rate is 4.5% and Type II error rate is 1%).

3.2. Application on functional brain imaging data

The application results on real fMRI data, which are the change points inferred for the functional network dynamics, are summarized in Table. 1. On average, over 90% of the 11 expected change points (defined by paradigm blocks) were detected within ± 5 time points. Those change points are defined as ‘‘aligned’’, summarized in the 2nd row in Table 1. Change points that are near the paradigm boundaries but outside the ± 5 time points range are defined as ‘‘partially aligned’’. The results indicate that the change points inferred by our model are largely in accordance with the block design, which validates its accuracy, as the functional dynamics is supposed to be responding to the changes of external stimulus.

Table 1 Summary of the results on real brain functional data.

Subject ID	1	2	3	4	5	6	7	8	9	10
Total number of change points detected	12	16	11	12	13	12	13	16	13	13
Change points aligned with boundaries	9	9	7	9	6	8	11	10	10	7
Change points partially aligned with boundaries	2	2	4	2	5	3	0	1	1	4
Change points not aligned with any boundaries	1	5	0	1	2	1	2	5	2	2

On the other hand, there were, on average, 2.2 change points detected by our model that could not be aligned with any block boundaries, usually appearing in the middle of the blocks. These are defined as ‘‘not aligned’’. Such change points are neither aligned nor partially aligned with any paradigm boundaries, and thus are different from the change points marked as red or grey in the previous discussion, yet could be meaningful and potentially to reflect the functional connectivity changes in the brain which happen within the temporal periods defined by the block design. In other words, although not frequent, functional connectivity dynamics might not always precisely follow the task design as reported in the literature [15]. By using data-driven methods like our model, one might detect such changes and utilize the change points to better infer more precisely the functional connectivity dynamics from the state-like fMRI temporal segments.

To further illustrate the importance and neuroscience implication of the change points detected, we applied the Peter and Clarke (PC) algorithm [13] to infer the high-order functional interactions between ROIs during the temporal segments defined by the change points. In this

preliminary study, we used the dataset from subject 4 as an example, as it has well-aligned change points with the task design as well as one change point that was detected in the middle of the 5th block (i.e., the 3rd activation block). The functional interaction patterns inferred from the five temporal segments as marked in the top row of Fig. 4 are visualized as the edges connecting ROIs on the cortical surface in Fig. 4. In the figure, the first two interaction patterns were inferred from the temporal segments 1 and 3, which were within the two activation blocks. The third interaction pattern was inferred from temporal segment 2, which was a baseline block. From Fig. 4, we could find that the interaction patterns from the activation periods are similar, while the baseline period has a different pattern. Interestingly, the fourth and fifth interaction patterns inferred from the temporal segment #4 and #5, where one single block was divided by the detected change point into two segments, show obvious different patterns. However, by applying the PC algorithm on the whole activation period, which is the combination of segments #4 and #5, we obtained the sixth pattern, which is totally different from the fourth pattern, indicating certain functional connectivity information was lost by analyzing a whole time period consisting of two intrinsically different temporal segments. Such differences demonstrate the importance of re-defining the brain state, not solely relying on the predefined paradigm design, but on the data-driven computational model that detects the abrupt change of the functional interaction, before performing further functional brain analysis.

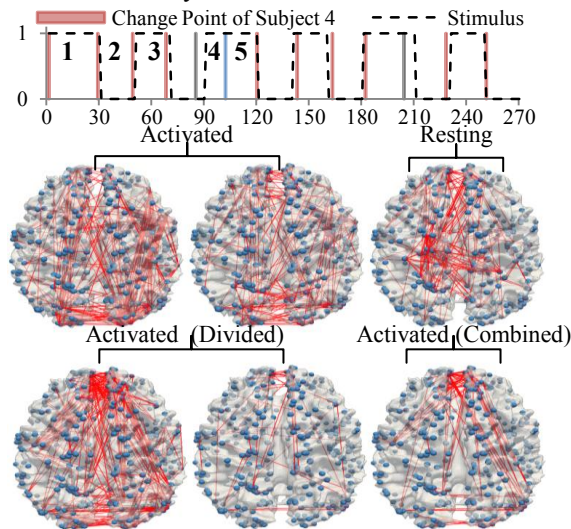


Fig. 4 Top: Change point detection results, shown as the red and blue bars of subject 4. The block designs of the OSPAN paradigm are overlaid as black dotted lines in the figure. Bottom: Visualizations of functional interaction patterns inferred from the five temporal segments defined by the change points in model results. The last (6th) pattern is the functional interaction from the whole activation period covering segment #4 and #5 in Fig. 4.

4. DISCUSSION AND CONCLUSION

In this study, we have presented a novel Bayesian inference model for change point detection in a multivariate time series dataset based on the interaction dynamics among variables. In this work, we mainly aim to apply this model on functional MRI imaging data to obtain a better understanding of the functional brain dynamics without any a priori knowledge. After extensive simulations which validated our proposed model, we have applied the model to real task-based fMRI data, and detected the change points largely corresponding to the brain dynamics in the block design. In the future, the preliminary study presented in this work could be further expanded to other fMRI datasets including resting-state data, as there remain unanswered questions regarding the boundaries between brain states and the functional dynamics varies across different subjects.

5. REFERENCES

- [1] Gilbert, C.D., et al., Brain States: Top-Down Influences in Sensory Processing,” *Neuron*, 54, pp. 677-696, 2007.
- [2] Majeed, W. et al., Spatiotemporal dynamics of low frequency BOLD fluctuations in rats and humans. *NeuroImage*, 2011.
- [3] Lindquist M.A., et al., Modeling state-related fMRI activity using change-point theory, *NeuroImage*, 35, 1125-1141, 2007.
- [4] Chang, C., et al., Time-frequency dynamics of resting-state brain connectivity measured with fMRI. *NeuroImage*, 2010.
- [5] Ramsey J.D., et al., Multi-subject search correctly identifies causal connections and most causal directions in the DCM models of the Smith et al. simulation study, *NeuroImage*, 58, 838-48, 2011.
- [6] Zhu, D., et al., DICCCOL: Dense Individualized and Common Connectivity-Based Cortical Landmarks. *Cerebral Cortex*, 2012.
- [7] Faraco, C.C., et al., Complex span tasks and hippocampal recruitment during working memory. *NeuroImage*, 2011.
- [8] Gelman A., et al., *Bayesian Data Analysis*, Second Edition, Chapman & Hall/CRC Texts in Statistical Science, 2003.
- [9] Liu J., *Monte Carlo Strategies in Scientific Computing*. Springer, 2001.
- [10] Smith, S.M., et al., Network modeling methods for FMRI. *NeuroImage*, 54 (2), 875–891. 2011.
- [11] Morgan, V.L., et al., 2004. Resting functional MRI with temporal clustering analysis for localization of epileptic activity without EEG. *NeuroImage* 21, 473-481.
- [12] Li X., et al., Detecting Brain State Changes via Fiber-Centered Functional Connectivity Analysis, in press, *Neuroinformatics*, 2013.
- [13] Meek, C., Causal inference and causal explanation with background knowledge, in *Proceedings of the Eleventh conference on Uncertainty in artificial intelligence* 1995.
- [14] Cribben, I., et al., Dynamic connectivity regression: Determining state-related changes in brain connectivity. *NeuroImage*, 61, pp. 907-920, 2012.
- [15] Zhang X., et al., Characterization of Task-free and Task-performance Brain States via Functional Connectome Patterns, in press, *Medical Image Analysis*, 2013.
- [16] Allen, E. A., et al., Tracking whole-brain connectivity dynamics in the resting state. *Cerebral Cortex*, 2012.